Origin of Diffusion Impedance at the Cathode of a Proton Exchange Membrane Fuel Cell

J. Mainka, G. Maranzana, J. Dillet, S. Didierjean, O. Lottin

This document appeared in

Detlef Stolten, Thomas Grube (Eds.):
18th World Hydrogen Energy Conference 2010 - WHEC 2010
Parallel Sessions Book 1: Fuel Cell Basics / Fuel Infrastructures
Proceedings of the WHEC, May 16.-21. 2010, Essen
Schriften des Forschungszentrums Jülich / Energy & Environment, Vol. 78-1
Institute of Energy Research - Fuel Cells (IEF-3)
Forschungszentrum Jülich GmbH, Zentralbibliothek, Verlag, 2010
ISBN: 978-3-89336-651-4

Origin of Diffusion Impedance at the Cathode of a Proton Exchange Membrane Fuel Cell

J. Mainka, G. Maranzana, J. Dillet, S. Didierjean, O. Lottin, LEMTA, Nancy University – CNRS, Nancy, France

Applied to Proton Exchange Membrane Fuel Cell (PEMFC), Electrochemical Impedance Spectroscopy (EIS) allows mainly the identification of the origin of potential losses. However, it can also be used to investigate the electrical properties of the fuel cell components, materials and interfaces, as well as the dependence of their performance on the operating conditions. As far as the diffusion impedance is concerned, one of the most common expressions is that of the finite Warburg element. It is based on simple assumptions: Fick's diffusion of oxygen, surface reaction, and a constant concentration at the gas channel boundary of the diffusion medium. However, as shown experimentally by Schneider et al. [1, 2], the consumption of oxygen along the air channel has a significant influence on the impedance values. Therefore, in order to improve the description of mass transfer, a decreasing oxygen concentration profile along the gas channel can be used as an alternative boundary condition, which leads to a slightly modified expression of the diffusion impedance. Then, starting from experimental spectra, it is possible to identify the impedances appearing in the fuel cell equivalent circuit and consequently, the mass transfer parameters at the cathode (effective diffusion coefficient and equivalent thickness). The values obtained with the usual expression of the Warburg impedance and with that taking account oxygen depletion can be significantly different [3].

1 Electrode Description

The Membrane-Electrode Assemblies (MEA) of PEMFC are complex composite systems made of various media with different physical properties. Thus, a well-adapted geometrical description of their structure is necessary to complete the physico-chemical description of mass transfer and reaction kinetics, all the more so since the limiting layer(s) in term of oxygen diffusion has (have) not been clearly identified yet. There exist different structural models of the electrodes in the literature, like agglomerate models [4-6] where the solid phase is a homogeneous mixture of catalyst (Pt), carbon powder and (possibly) polymer electrolyte forming either cylindrical [7-8] or spherical [9-13] particles. Actually, two descriptions of the solid phase coexist in the literature. In the first case, the agglomerate consists in a mixture of carbon, Pt and electrolyte [4, 7]. The second case corresponds to the description first proposed by Springer [5] and Raistrick [6] where the agglomerate is a mixture of carbon powder and catalyst particles only whereas the electrolyte is assumed to cover the surface of the pores. The catalytic sites are at the interface between the electrolyte and the agglomerates, which corresponds to a surface description of the active layer. Before accessing the active layer, oxygen passes successively through the GDL, through the pores of the electrode, and finally through the thin electrolyte layer coating the carbon and platinum agglomerate. This description is chosen for the interpretation of the impedance spectra.

Since the cathode is the place of water production, the ionic resistance of the well-hydrated polymer can be neglected. The other main hypotheses of the one-dimensional mass transfer model are: the fuel cell is isotherm and isobar, ohmic drops in the active layer and in the GDL are neglected, mass transfer of O_2 and H_2O is assumed to occur only by diffusion in the pores of the active layer and the GDL, water diffusion through the solid phase of the active layer is not considered.

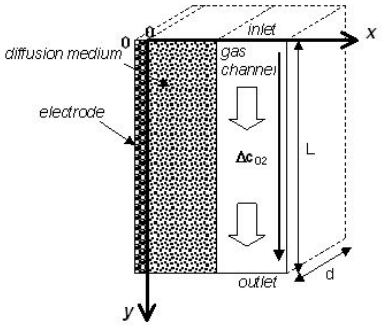

Figure 1: Schematic representation of the pseudo-2D diffusion model. Oxygen concentration variation occurs in the channel between y = 0 and y = L. Oxygen diffusion is considered only in the x-direction, perpendicularly to the electrode surface. The electrode surface is given by *L* × *d*.

In order to take into account the variation in oxygen concentration along the gas channel in the pseudo-2D model (*Figure 1*), three more hypotheses are made: mass transfer resistance in the gas channel is neglected, time variations of the oxygen concentration in the channel are neglected, the Tafel slope *b* is constant between the inlet and the outlet of the air channel.

The faradaic current density $j_f(y)$ and the oxygen concentration $c_{O2}(x,y)$ vary as functions of the y coordinate (Figure 1). *J* is the cell average current density:

$$J = \frac{I}{Ld} = \frac{1}{L}\int_0^L j_f(y)\,dy$$

For convenience, we consider the absolute value of the activation overpotential and the faradaic current density at the cathode: $j_f(y), \eta_{act} > 0$. φ_{O_2} and φ_{H_2O} denote the fluxes in the y direction (in the air channel, in *Mol/s*) while N_{H_2O} and N_{O_2} denote the flux densities in the x direction (in the gas diffusion layer, in *Mol/s/m²*). The molar fluxes of oxygen φ_{O_2} and water φ_{H_2O} in the channel depend also on their y-position. Thus, the molar flux of oxygen $\varphi_{O_2}(y)$ corresponds to that at the inlet of the gas channel minus the amount consumed at the cathode:

$$\varphi_{O2}(y) = \varphi_{02}^{in} - \frac{d\int_0^y j_f(y)\,dy}{4F}$$

Mass transfer along the x direction is assumed to occur only by diffusion, which means that the global molar flux density in x direction $N_{H_2O} + N_{O_2}$ has to be null (Figure 1). This is a particular case that happens when only half of the water produced at the cathode is evacuated toward the air channel ($N_{H_2O} = j_f(y)/4F$), which compensates for the oxygen flux N_{O_2} in the opposite direction[1]. The other half of water produced by the fuel cell as well as the molecules flowing from anode to cathode under the effect of the electro-osmotic drag must diffuse through the membrane under the effect of a concentration gradient. The water flux along the gas channel φ_{H_2O} (in the *y* direction) is a function of *y*, given by:

$$\varphi_{H20}(y) = \varphi_{H20}^{in} + \frac{d\int_0^y j_f(y)dy}{4F}$$

The oxygen molar ratio along the GDL/gas channel interface $(x = \delta)$ is given by:

$$c_{02}(x = \delta, y) = \frac{S_{02} - \frac{d\int_0^y j_f dy}{I}}{S_{02}(1+H)} c_{02}^0$$

Where $S_{02} = \frac{\varphi_{02}^{in}}{I/4F}$ is the oxygen stoichiometric ratio, $H = \frac{\varphi_{H20}^{in}}{\varphi_{02}^{in} + \varphi_{N2}}$ is the absolute inlet humidity and $c_{O2}^0 = \frac{P}{5RT}$ is the inlet concentration of oxygen in dry air.

Strictly speaking, mass transport of oxygen through the pores of the diffusion media in a PEMFC is described by Stefan-Maxwell equations. However, since the binary diffusion coefficients of O_2/H_2O and O_2/N_2 are close to each other, it seems reasonable to use Fick's 1st law. Assuming that the electrochemical reaction takes place only at the active layer/membrane interface (*x = 0*), the 1st Fick's law can be written:

$$N_{O2}(y) = -D_{eff} \left.\frac{\partial c_{O2}}{\partial x}\right|_{\substack{x=0 \\ y}}$$

The diffusion media being porous, it is necessary to use an effective diffusion coefficient D_{eff} taking into account their porosity *ε* and possibly, the presence of Knudsen diffusion. The most common expressions obey Archie's law [14]: $D_{eff} = D\varepsilon^m$, where *m* is an exponent varying between 1.5 and 4. In the case of a *3D* medium, there is a wide consensus for using *m = 3/2*, which corresponds to the differential effective medium approximation introduced by

[1] Note that the question of the validity of the Warburg diffusion impedance in PEM fuel cells does not seem to have been fully addressed yet considering that these operating conditions are not common: the water net drag coefficient can differ significantly from 0.5.

Bruggeman [14-15]. *m = 3/2* is probably appropriate for the active layers, in which the orientation of the solid phase does not follow a privileged direction. In the gas diffusion layers however, the solid phase can be considered as two-dimensional since the carbon fibres are mainly parallel to the electrodes. In this case, the result of the differential effective medium theory is *m = 2* [15]. Knudsen diffusion must be considered in the active layers only, using for instance the Bosanquet formula $\frac{1}{D} = \frac{1}{D_{mol}} + \frac{1}{D^K}$, with $D_i^K = \frac{1}{3} d_{pore} \sqrt{\frac{8RT}{\pi M_i}}$.

Adding a small sinusoidal perturbation $\Delta j_f(y,t)$ to the mean (*DC*) current density $\langle j_f(y) \rangle_t$ makes the oxygen concentration $c_{O2}(x,y,t)$ fluctuating around its steady-state value $\langle c_{02}(x=\delta,y) \rangle_t$ with the same frequency. Solving the diffusion equations with the right boundary conditions allows to express the diffusion impedance as a function of *y*:

$$Z_{c02}^{2D}(y) = R_d^{2D} \frac{\tanh\left(\sqrt{iw\tau_d}\right)}{\sqrt{iw\tau_d}} \text{ with } R_d^{2D} = \frac{b\delta}{4FD_{eff}\langle c_{02}(x=0,y)\rangle_t} \text{ and } \tau_d = \frac{\delta^2}{D_{eff}}.$$

The expression of the pseudo-2D diffusion impedance is close to that of the finite Warburg element. It can be used in the usual Randles equivalent circuit [16] of a whole fuel cell (Figure 2).

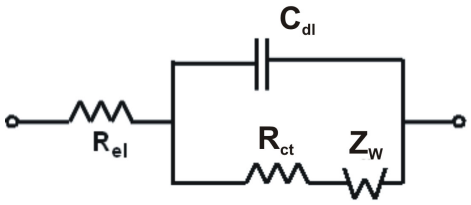

Figure 2: MEA equivalent electrical circuit according to Randles [16].

2 Experimental Setup

The measurements are carried out with a single cell where the current collection is segmented on the cathode side thanks to a set of *18* gold plated brass strips spaced at intervals of *1 mm* (Figure 3). This design makes it possible to perform locally resolved impedance spectroscopy. The current collectors are embedded in a PMMA plate and they delimit a serpentine air channel (of section *0.7 x 1.0 mm²*) on the cathode side of the cell. The hydrogen channel is symmetric to the air channel. The GDL is a *190 µm* thick carbon fibre paper (*Toray™ TGP-H-060*) with a no-compressed porosity $\varepsilon = 0.78$. The MEA (of active area *A = 7.87 cm²*) consists of a PFSA polymer membrane of thickness $\delta_m = 30\ \mu m$ and catalytic layers ($\delta_{cat} \approx 10\ \mu m$) with an average Pt loading of *0.406 mg cm⁻²* at the anode and *0.385 mg cm⁻²* at the cathode. The fuel cell is fed in co and counter-flow (at *1 atm*) by dry hydrogen with a stoichiometric ratio $S_{H2} = 1.2$ and by humidified air with a stoichiometric ratio $S_{air} = 3$. The air is humidified up to about *74 % RH*. All impedance measurements are performed in galvanostatic mode in a frequency range of *0.4 Hz* to *200 Hz* with a peak-to-peak sinusoidal perturbation of *5 %* of the cell current intensity. Global and local impedance

measurements are performed using a passive electronic circuit where each of the 18 brass strips is connected to a *10 mΩ* shunt resistance.

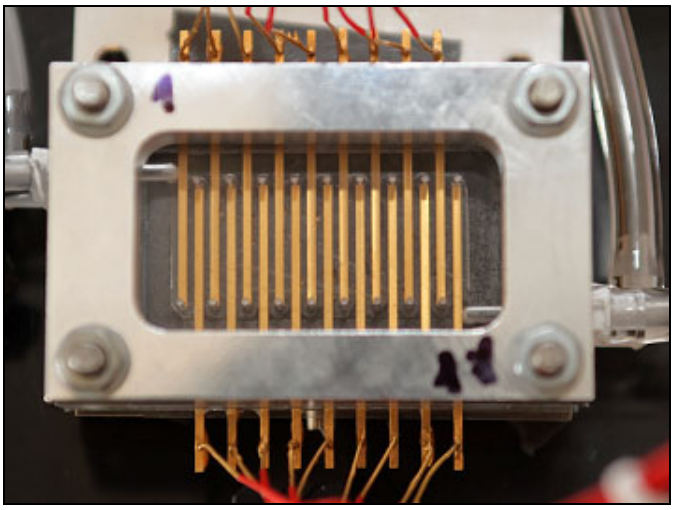

Figure 3: Instrumented cell.

3 Experimental Results

All the results presented below were obtained in identical conditions with a current density fixed to 0.5 Acm^{-2}. Figure 4 shows the local impedance spectra obtained for a gas supply in co-flow (left) and counter-flow (right). The air inlet corresponds to the first segment. In both cases, a second low frequency loop appears progressively along the air channel. This could lead to the conclusion that mass transfer in the GDL or in the active layer becomes limiting but a more detailed analysis carried out after identification of the impedance parameters is necessary. Figure 5 shows the profiles of the diffusion impedance parameters (R_d^{2D} , τ_d) identified starting from the Randles equivalent circuit (Figure 2).

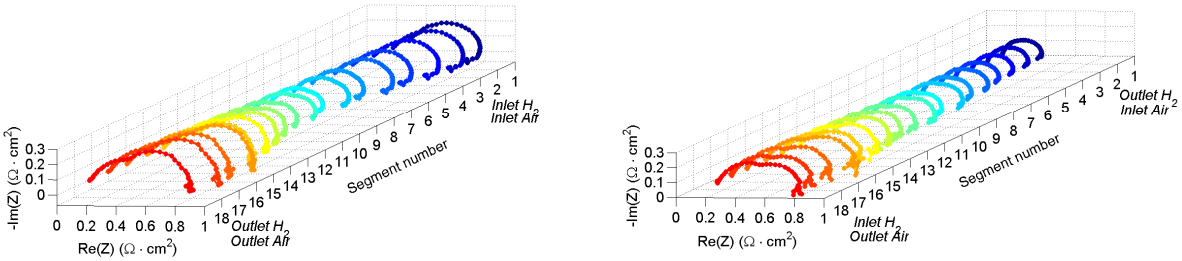

Figure 4: Local impedance spectra in co-flow (left) and counter-flow (right).

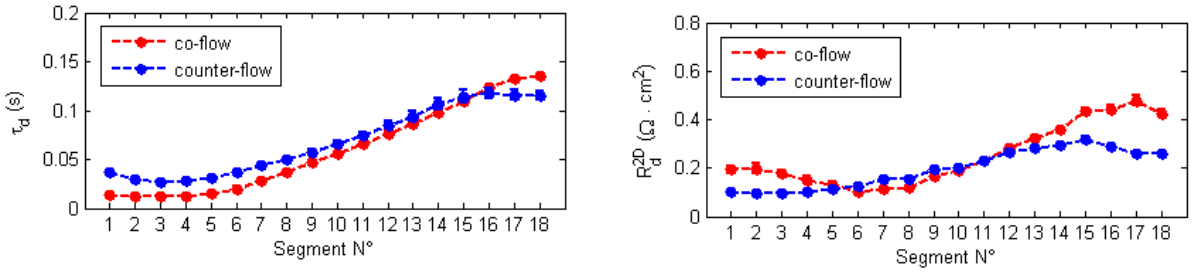

Figure 5: Profiles of the characteristic diffusion time τ_d and the diffusion resistance R_d^{2D}.

The diffusion time τ_d (Figure 5, left) increases progressively along the air channel in co-flow and counter-flow modes. At the air inlet, τ_d is slightly larger in counter-flow than in co-flow, whereas at the channel outlet, the opposite is observed. This difference could be interpreted in term of water content, the air channel inlet being less humidified in co-flow whereas the amount of water is more important near the outlet. The comparison of the profiles of the diffusion resistance R_d^{2D} (Figure 5, right) leads to the similar conclusion but the highest value observed near the air channel inlet in co-flow remains more difficult to explain: one possible interpretation could be that dry conditions reduce oxygen diffusion in the thin electrolyte layer that covers the active sites. However, these tentative conclusions require confirmation.

The values of the diffusion length δ, the effective diffusivity D_{eff}, and the porosity ε can be derived from R_d^{2D} and τ_d. Their profiles are plotted in Figure 6.

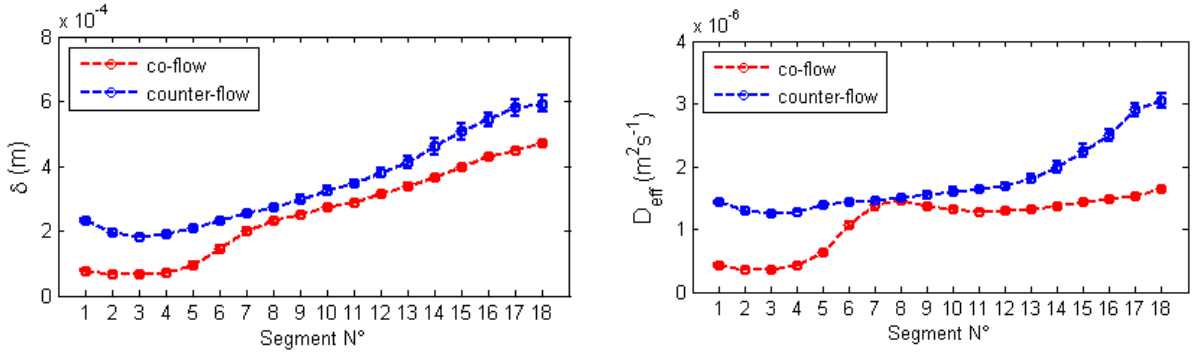

Figure 6: Profiles of the diffusion thickness δ and the effective diffusivity D_{eff} along the air channel.

The diffusion length δ (Figure 6, left) increases continuously along the air channel on co-flow and counter-flow modes but with lower values in the first case. This does not allow any conclusion about the local water content. δ ranges from *77 µm* to *593 µm*, which is far above the typical thickness of catalyst layers (≈ *10 µm*). This suggests that at the limiting media for mass transfer is rather the GDL ($\delta_{GDL} = 190\,\mu m$) but there could be many reasons for the increase in δ along the air channel: 2D diffusion in the GDL below the current collectors, or mass transfer resistance or propagation of the oscillations of oxygen concentration in the channel [1, 2]. As far as the profile of the effective diffusion coefficient is concerned

(Figure 6, right), the increase observed along the air channel seems to be in contradiction with a possible accumulation of liquid water in the pores of the gas diffusion or active layer. However, this increase could also be explained by phenomena occurring upstream in the channel. The numerical values of D_{eff} suggest that if the limiting media were the GDL only or the active layer only, their effective porosity (accounting for the presence of liquid water) would be comprised between 0.2 and 0.6, and 0.2 and 0.35, respectively. Once again, these values do not allow to discriminate between the contribution of the gas diffusion layer and of the active layer to the impedance diffusion. However, the diffusion does not seem to take place in liquid phase, which would yield diffusivities of about $D_{eff} \approx 10^{-11} m^2 s^{-1}$.

4 Conclusion

EIS is frequently used to investigate the origin of the mass transfer impedance in cathode gas diffusion and active layers. However, the expression of a finite Warburg element used for analysing impedance spectra is obtained assuming that the oxygen concentration at the gas channel/gas diffusion layer interface is constant. This hypothesis is much constraining when the gas stoichiometry is low, and it could lead to wrong estimates of mass transfer parameters characterising the diffusion media. An alternative to this expression is proposed: considering gas consumption along the gas channel, which allows furthermore to investigate variations in local impedance spectra and in the diffusion kinetics along the air channel. In this paper, we presented some preliminary results identified from local impedance spectra. They show that oxygen transfer takes place in gaseous phase but they do not allow to discriminate between the contribution of the gas diffusion layer and of the active layer to the impedance diffusion. Furthermore, high values of the diffusion thickness were observed (up to about 3 times the actual GDL thickness). This could be explained either by gas diffusion below the channel rib or by oscillations of the oxygen concentration upstream in the air channel.

References

[1] I.A. Schneider, S.A. Freunberger, D. Kramer, A. Wokaun and G.G. Scherer, J. Electrochem. Society 154 (2007) B383-B388.

[2] I.A. Schneider, D. Kramer, A. Wokaun and G.G. Scherer, J. Electrochem. Society 154 (2007) B770-B782.

[3] J. Mainka, G. Maranzana, J. Dillet, S. Didierjean, O. Lottin, ECS Transactions, Analytical Electrochemistry (General), Volume 19, October 2009.

[4] F. Gloaguen, P. Convert, S. Gamburzev, O. A. Velev and S. Srinivasan, Electrochimica Acta 43 (1998) 3767-3772.

[5] T. E. Springer, I. D. Raistrick, J. Electrochemical Soc. 136 (1989)1594-1603.

[6] I. D. Raistrick, Electrochimica Acta 35 (1990) 1579-1585.

[7] J. Ramousse, J. Deseure, O. Lottin, S. Didierjean, D. Maillet, J. Pow. Sources 145 (2005) 416-427.

[8] M. Bautista, Y. Bultel, P. Ozil, I. Chem. Eng. 82 (2004) 907-917.

[9] N. P. Siegel, M.W. Ellis, D.J. Nelson, M.R. von Spakovsky, J. Pow. Sources 115 (2003) 81-89.

[10] S.J. Lee, S. Mukerjee, J. McBreen, Y.W. Rho, Y.T. Kho, T.H. Lee, Electrochimica Acta, 43 (24) (1998) 3693-3701.

[11] W. Sun, B.A. Peppley, K. Karan, Electrochimica Acta, 50 (2005) 3359-3374.

[12] F. Jaouen, G. Lindbergh, K. Wiezell, J. Electrochemical Soc. 150 (2003) A1711-A1717.

[13] K. Broka, P. Ekdunge, J. App. Electrochemistry, 27(2) (1997) 117–123.

[14] S. Torquato, Random Heterogeneous Materials: Microstructure and Macroscopic Properties, Springer (2002).

[15] H. C. Bruggeman, Berechnung verschiedener Physikalischer Konstanten von heterogenen Substanzen, Ann. Physik (Leipzig) 24, 636-679 (1935).

[16] J.E.B. Randles, Discuss. Faraday Soc., 1, 11 (1947).